Langmuir

Letter

pubs.acs.org/Langmuir

Carbodiimide/NHS Derivatization of COOH-Terminated SAMs: Activation or Byproduct Formation?

Francisco Palazon,[†] Cindy Montenegro Benavides,[†] Didier Léonard,[‡] Éliane Souteyrand,[†] Yann Chevolot,*[,†] and Jean-Pierre Cloarec*[,†,§]

[†]Université de Lyon, Institut des Nanotechnologies de Lyon, Site École Centrale de Lyon, CNRS UMR 5270, 36 Avenue Guy-de-Collongue, 69134 Écully, France

[‡]Université de Lyon, Institut des Sciences Analytiques, Université Claude Bernard Lyon 1/CNRS/ENS de Lyon, CNRS UMR 5280, 5 rue de la Doua, 69100 Villeurbanne, France

[§]Laboratoire Nanotechnologies & Nanosystèmes, UMI 3463 CNRS, UdeS, INSA de Lyon, ECL, UJF, CPE Lyon, Université de Sherbrooke, 3000 Boulevard de l'Université, Sherbrooke, Québec J1K 0A5, Canada

Supporting Information

ABSTRACT: COOH-terminated self-assembled monolayers (SAMs) are widely used in biosensor technology to bind different amine-containing biomolecules. A covalent amide bond, however, can be achieved only if the carboxylic acids are activated. This activation process usually consists of forming an *N*-hydroxysuccinimidyl ester (NHS-ester) by consecutively reacting carboxylic acids with a carbodiimide and NHS. Though many papers report using this method,[1−8] the experimental conditions vary greatly between them and chemical characterization at this stage is often omitted. Evidence of an efficient activation is therefore rarely shown. Furthermore, recent publications[9−11] have highlighted the complexity of this process, with the possible formation of different byproducts. In this paper, we have conducted a study on NHS activation under different conditions with chemical characterization by polarization-modulation infrared reflection−absorption spectroscopy (PM-IRRAS) and time-of-flight secondary ion mass spectroscopy (ToF-SIMS). Our results indicate that the nature of the solvent and carbodiimide and the reactant concentrations play crucial roles in activation kinetics and efficiency.

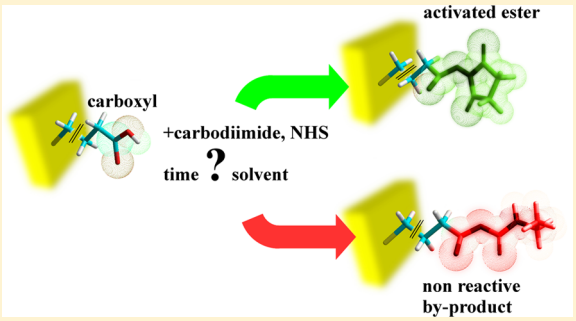

INTRODUCTION

Self-assembled monolayers are widely used to attach biomolecules to gold.[1,2,12,13] Among the different headgroups available for immobilizing biomolecules, carboxylic acids (COOH) are commonly chosen for their ability to bind amine groups (NH_2) that are present in proteins, peptides, or amino-functionalized oligonucleotides (DNA, RNA, aptamers, etc.). COOH and NH_2, being oppositely charged in most biological buffers such as PBS (pH 7.4), can interact electrostatically without further derivatization. However, if covalent binding is desired, it is necessary to activate the COOH groups. Activation commonly consists of forming a reactive NHS-ester by a two-step reaction between the acid and a carbodiimide to form *O*-acylurea followed by a reaction between *O*-acylurea and NHS to yield the activated NHS-ester[9] (see Scheme 1).

Given the widespread use of this methodology,[1−8] it could be thought that a well-established protocol leading to efficient activation exists. However, as noted by others,[9] an important number of parameters vary greatly between studies. Indeed, activation may be performed in water with *N*-(3-(dimethylamino)propyl)-*N*′-ethylcarbodiimide (EDC)[1−5] but also in organic solvents such as dimethyl sulfoxide (DMSO)[6] or tetrahydrofuran (THF)[7] with other carbodiimides such as *N*,*N*′-dicyclohexylcarbodiimide (DCC)[6,8] or *N*,*N*′-diisopropylcarbodiimide (DIC).[7] Carbodiimide and NHS concentrations and the activation time are also found to vary greatly.[1,6,14] Furthermore, there is often no chemical characterization at this stage to prove the efficiency of the activation process. It should be noted that achieving the immobilization of a protein does not constitute proof of an efficient activation, as proteins can be easily physisorbed and may actually bind to a greater extent on nonactivated COOH rather than on NHS-ester.[15]

Recent publications[9−11] have highlighted the fact that the activation of carboxylic acids on SAMs is a complex reaction (see Scheme 2) which can lead not only to the desired NHS-ester formation (reaction 3) but also to different byproducts such as *N*-acylurea (reaction 1) and anhydrides (reaction 2):

In addition to the different possible reactions reported in Scheme 2, it should be noted that the hydrolysis of different

Received: January 31, 2014
Revised: April 10, 2014
Published: April 10, 2014

   dx.doi.org/10.1021/la5004269 | *Langmuir* 2014, 30, 4545−4550

Scheme 1. Activation of Carboxylic Acids by Carbodiimide and NHS without Byproducts[9]

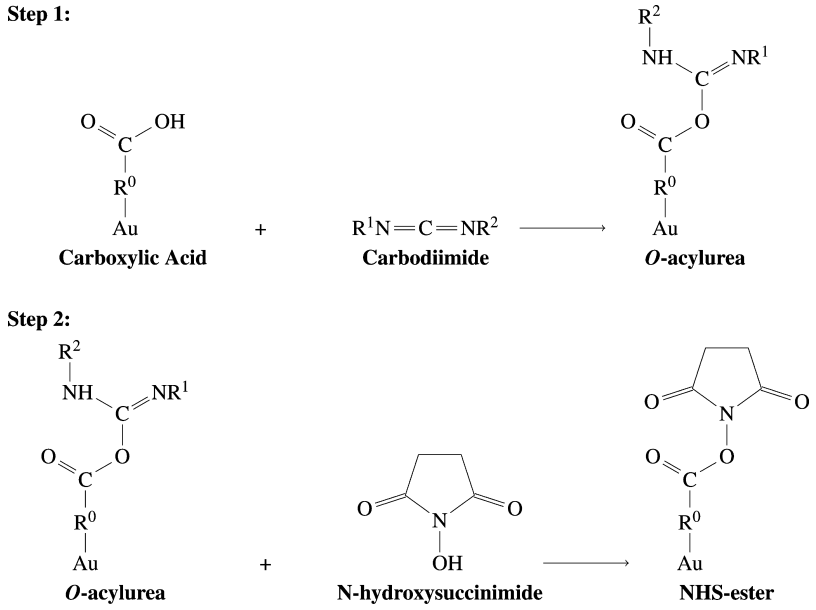

Scheme 2. Possible Derivatizations of *O*-Acylurea in the Presence of NHS, Including the Expected NHS-Ester and Main Byproducts *N*-Acylurea and Anhydride[9]

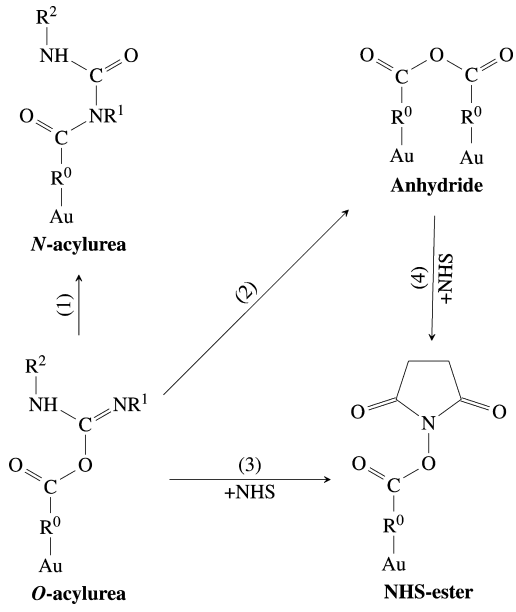

species can furthermore make the overall reaction scheme more complex. Most importantly, carboxylic acids can be regenerated at the surface through the hydrolysis of *O*-acylurea[16] or NHS-ester.[17] Additionally, the hydrolysis of carbodiimides and *O*-acylurea can also produce other byproducts such as urea derivatives.[16,18]

Sam et al.[9] showed the impact of EDC and NHS concentration on the efficiency of the activation process and the appearance of the aforementioned byproducts, with a systematic infrared characterization of the different terminal groups at the surface, albeit not providing information about the kinetics of the different reactions.

Time-of-flight secondary ion mass spectroscopy (ToF-SIMS) and polarization-modulation infrared reflection absorption spectroscopy (PM-IRRAS) are surface-sensitive methods specially suited for this study. Indeed, as shown by Frey et al.,[14] the activation process can be monitored by the presence of an infrared absorption peak at ca. 1820 cm^{-1}. It should be noted that during the activation, other bands appear at ca. 1785 and 1745 cm^{-1}, with the latter being the most prominent one. However, these two are linked to NHS (be it covalently bonded or just adsorbed) and are therefore not representative of the activated ester (NHS covalently bonded to the acid head-group).

In this paper, we have conducted a methodological study on the activation process of 1-mercapto-11-undecanoic acid (MUA) SAMs on gold under different conditions, characterized by PM-IRRAS and ToF-SIMS. The following results highlight the different esterification and byproduct formation kinetics depending on the nature of the carbodiimide and corresponding solvent (EDC in water vs DIC in THF) as well as the reactant concentrations.

EXPERIMENTAL SECTION

Chemicals. 1-Mercapto-11-undecanoic acid 95% (MUA), *N*-(3-(dimethylamino)propyl)-*N*′-ethylcarbodiimide hydrochloride (EDC) 99%, *N*-hydroxysuccinimide (NHS) 97%, *N*,*N*′-diisopropyl-carbodiimide (DIC) 98%, ethanol 99.8%, and THF 99% were purchased from Sigma-Aldrich.

Gold Functionalization. Gold samples (200 nm thick) were prepared by e-beam evaporation onto silicon wafers with an adhesion layer of chromium (5 nm thick). The deposition rate for the gold layer was 2.5 Å/s. Substrates were cleaned with UV/ozone for 30 min, and the surface was checked with PM-IRRAS before functionalization. SAMs were formed by immersing the samples for 4 h in 10 mM solutions of MUA in slightly aqueous ethanol (95/5 v/v), previously degassed under nitrogen. This solvent was chosen in order to limit the well-known deprotonation of carboxylic acids that occurs in pure ethanol[19−22] (see the Supporting Information for further evidence). The samples were then washed in fresh ethanol/water (95/5 v/v) for 2 × 5 min under sonication to remove potentially adsorbed multilayers and soaked in ultrapure water for another 5 min before drying with nitrogen.

MUA Activation. Previously formed SAMs were activated with a mixture of EDC/NHS in ultrapure water or DIC/NHS in THF dried over molecular sieves, both at two different concentrations: 20 mM +

dx.doi.org/10.1021/la5004269 | *Langmuir* 2014, 30, 4545−4550

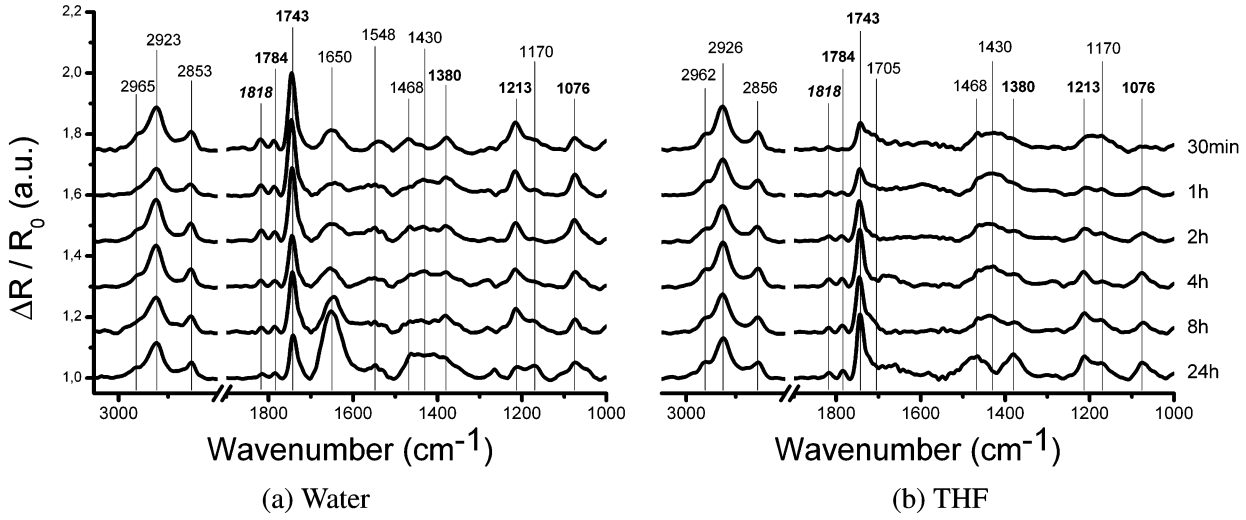

Figure 1. Samples activated in (a) water and (b) THF with 100 mM concentrations of the corresponding carbodiimide and NHS. Characteristic NHS absorption wavenumbers are written in bold, and the 1818 cm^{-1} peak, characteristic of NHS-ester, is written in bold and italic.

20 mM and 100 mM + 100 mM ([carbodiimide] + [NHS]). The samples were taken out of the solution at different times (30 min and 1, 2, 4, 8, 24 h), washed in ultrapure water for 2 × 5 min under sonication to remove potentially adsorbed multilayers, dried with nitrogen, and characterized by PM-IRRAS.

Infrared Characterization. Characterization of the surface was carried out by polarization-modulation infrared reflection−absorption spectroscopy (PM-IRRAS, also referred to in the literature as PM-RAIRS and PM-FTIRRAS). The theory of PM-IRRAS has been explained elsewhere.[23,24] In short, in a PM-IRRAS setup, as opposed to conventional IRRAS, the incident-beam polarization is switched from p to s by a photoelastic modulator (PEM) at a given high frequency. This makes it possible to acquire two different signals, corresponding to the difference and sum reflectivities: $|R_p - R_s|$ and $R_p + R_s$. The ratio $\Delta R/R_0 = ((|R_p - R_s|)/(R_p + R_s))$ constitutes a spectrum of the surface, without the need to acquire a background spectrum as in conventional IRRAS. However, the PEM is not efficient at all wavenumbers simultaneously, which results in a low-frequency superimposition on the spectrum corresponding to a second-order Bessel function.[23] Thus, the baseline was corrected each time by dividing the experimental spectrum by a spline line fitted to the regions where no peak was expected.[19,24] This method is often used as it gives the correct relative peak intensities albeit yielding arbitrary units for the y axis.[12,19]

We used a Nicolet 6700 FTIR spectrometer from Thermo Scientific coupled to a Hinds Instrument PEM-100 ZnSe photoelastic modulator driven at 50 kHz (polarization switch from p to s at 100 kHz). The wavenumber of optimum detection (wavenumber at which the PEM works as an oscillating half-wave plate) was set at 2000 cm^{-1} for a full scan (4000−800 cm^{-1}), with emphasis on the C═O region. All spectra were acquired at 8 cm^{-1} resolution and an angle of incidence of 85° for optimum sensitivity on gold. Further analysis of the spectra were performed with TQ Analyst software and Origin 8.0. The evaluation of the activation process was made by measuring the area of the NHS-ester peak with baseline correction between 1835 and 1802 cm^{-1} except for samples functionalized in water after 24 h, where the peak was slightly shifted to the right (baseline taken between 1829 and 1800 cm^{-1}).

ToF-SIMS Characterization. Time-of-flight secondary ion mass spectrometry (ToF-SIMS) measurements were performed with a Physical Electronics TRIFT III instrument (Physical Electronics, Chanhassen, MN) operated with a pulsed 22 Au^+ ion gun (ion current of 2) rastered over a 300 μm × 300 μm area. The ion dose was kept below the static conditions limits. Data were analyzed using WinCadence software. Mass calibration was performed on hydrocarbon secondary ions. The maximum deviation between the measured m/z for ToF-SIMS peaks and the exact m/z for the corresponding assigned ions was 20 milliatomic mass units. Data were normalized to the total intensity minus the $H^{\pm}$ intensity because of its low reproducibility and expressed as a percentage:

$$I_{norm} = \frac{I}{I_{total} - I_{H^{+/-}}} \times 100$$

RESULTS AND DISCUSSION

For the following discussion of PM-IRRAS results, the most relevant infrared vibration modes and wavenumbers can be found in the Supporting Information.

Figure 1 shows the evolution of the surface upon activation in water and THF at concentrations of 100 mM in carbodiimide and NHS.

Many features can be distinguished in these spectra, some of which relate to the presence of NHS: $\nu_{C=O}$ triplet at 1818, 1784, and 1743 cm^{-1}; ν_{NCO}^{sym} at 1076 cm^{-1}; ν_{CNC}^{assym} at 1213 cm^{-1}; and ν_{CNC}^{sym} at 1380 cm^{-1} (with a possible contribution from $\delta_{CH_3}^{rock}$ that will be discussed later).

To quantify the activation of carboxylic acids, it is tempting to consider the ca. 1743 cm^{-1} band, as it is the most prominent one in succinimidyl esters. However, this band is not characteristic of the activated ester as it is also present in potentially physisorbed succinimide. Furthermore, it can be overlapped by the $\nu_{C=O}$ of free carboxylic acids. Therefore, we have quantified the area under the 1818 cm^{-1} band, characteristic of the NHS-ester. It should be noted that this attribution implies the lack of anhydride at the surface, which is consistent with the lack of a peak at 1750 cm^{-1} and the similar evolution and widths of the 1818 and 1784 cm^{-1} peaks which suggest a unique contribution for both.[9] Moreover, this is consistent with the literature[9] that suggests that direct NHS-ester formation is dominant in comparison to the anhydride intermediate at such high concentrations of NHS, although an anhydride intermediate may have been formed in the very early stages (first few minutes) of the reaction[11] and therefore not detected here. Very different behaviors were shown depending on the solvent (and corresponding carbodiimide), the concentration, and the time. These are summarized in Figure 2 below.

One can see that activation in water occurs very fast (<30 min) at both concentrations and then decays (immediately at

dx.doi.org/10.1021/la5004269 | Langmuir 2014, 30, 4545−4550

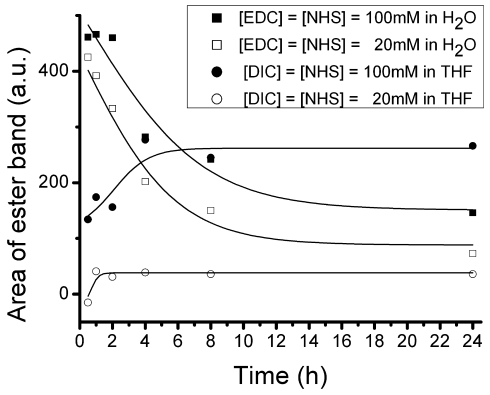

Figure 2. Area of the 1818 cm^{-1} peak for different solvents/carbodiimides, concentrations, and times. Below a value of 150 au, the peak is barely noticeable.

20 mM; after 2 h at 100 mM) to yield almost no activated esters at 24 h. This can be explained by the competing hydrolysis of the ester in water.[17]

In THF, however, activation is evidenced only for the higher concentration (100 mM) and after ca. 1 h. After 4 h, a more or less constant level is maintained until 24 h (no measurements were performed at times greater than 24 h).

It should be noted from Figure 1 that the peaks corresponding to the NHS (cycle) (1784, 1743, 1076, 1213, and 1380 cm^{-1}) evolve in the same way as the NHS-ester peak at 1818 cm^{-1}, which suggests that there is no adsorbed NHS at the surface.

Concerning the other peaks present in Figure 1 (activation in water and in THF), the bands at 2926−2923, 2856−2853, and 1468 cm^{-1} can be attributed to vibrational modes of the alkyl chain ($\nu^{assym}_{CH_2}$, $\nu^{sym}_{CH_2}$, and δ_{CH_2}, respectively), which are independent of the activation process and therefore more or less constant in both cases.

The region between 1743 and 1468 cm^{-1} is more interesting as it presents clear differences between water and THF as well as different evolutions in each sample. First we can see that two bands are present at 1650 and 1548 cm^{-1} in the sample activated in water and not in THF. These bands are strongly evocative of amide I and II vibrations which suggest the presence of the *N*-acylurea byproduct. A contribution from δ_{H_2O} of adsorbed water may also be possible, as noted by others in similar studies.[11,19] Such an increase in hydrophilicity would be consistent with the hydrolysis of NHS-ester into carboxylic acids.[11] However, the principal assignment of this peak to *N*-acylurea seems more likely, considering the following characterization by ToF-SIMS as well as the fact that, in order for physisorbed water to have a significant signal by PM-IRRAS, most water molecules should have a precise orientation with regard to the surface (PM-IRRAS is insensitive to isotropic dipoles). In THF, no water or amide bands could be detected. In contrast, the carbonyl region was found to be much broader (1743−1705 cm^{-1}), which suggests unreacted carboxylic acids at the surface. This is consistent with the slower kinetics of esterification in this solvent.

ToF-SIMS measurements were carried out on these surfaces for further analysis of the final products (see Figure 3), and normalized intensities ($I_{norm} = (I/(I_{total} - I_{H^+}) \times 100$) of various characteristic ions were calculated. Figure 3a,b indicates the detection on both surfaces of CN^- at m/z = 26 (3.87% in

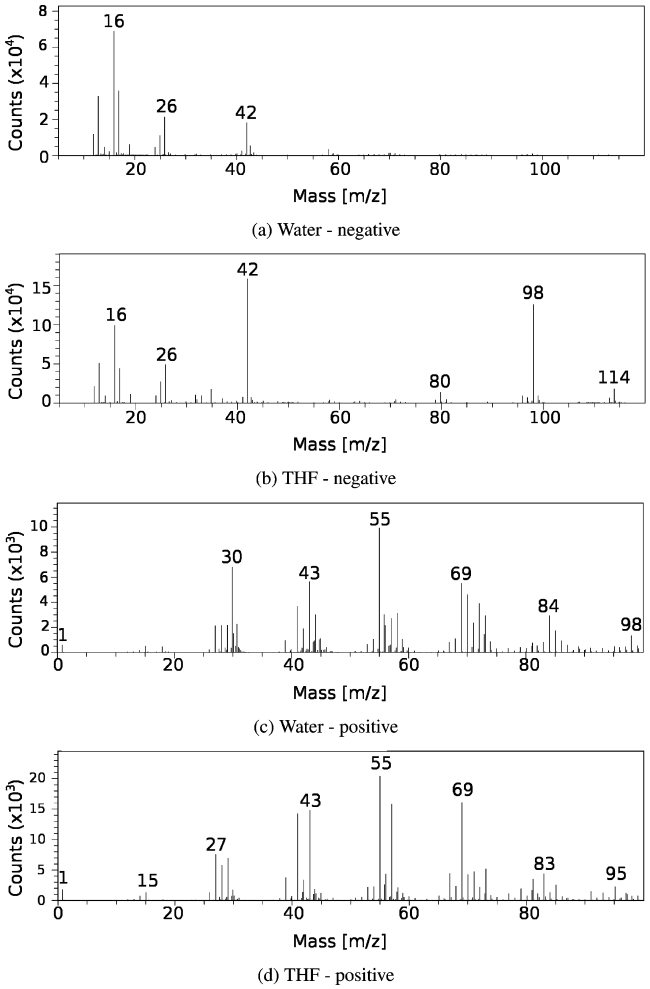

Figure 3. Negative (a and b) mode and positive (c and d) mode ToF-SIMS spectra of samples activated in water (a and c) and THF (b and d) after 24 h in the ranges of m/z = 5−120 (negative mode) and m/z = 0−100 (positive mode).

THF and 6.85% in water) and of CNO^- at m/z = 42 (11.72% in THF and 5.82% in water). However, other signatures indicate a different nitrogen-based surface chemistry. Indeed, in THF we can observe an intense peak at m/z = 98 (9.48%) which can be assigned to $C_4H_4NO_2^-$ of NHS.[25] This represents only 0.35% on the sample activated in water. The m/z = 114 peak in Figure 3b can also be assigned to an NHS moiety ($C_4H_4NO_3^-$)[25] and is absent in Figure 3a. Conversely, in positive mode (Figure 3c,d), we can see a main difference at m/z = 30 which can be assigned to CH_3NH^+. This represents 5.54% in water versus 0.75% in THF. This and the m/z = 84 peak ($C_4H_6NO^+$) are consistent with the structure of EDC-derivatized *N*-acylurea. These peaks could also originate from other EDC derivatives including *O*-acylurea, physisorbed EDU (EDC urea derivative from hydrolysis[18]), and plain unreacted EDC. However, the assignment to *N*-acylurea seems more reasonable given the high reactivity of *O*-acylurea and the thorough washing under sonication as well as the previously mentioned amide bands in the PM-IRRAS spectra. In summary, ToF-SIMS analysis confirms the higher amount of NHS on the sample activated in THF after 24 h compared to that activated in water and the predominance of an EDC-derivatized byproduct assigned to *N*-acylurea on the latter.

dx.doi.org/10.1021/la5004269 | *Langmuir* 2014, 30, 4545−4550

Furthermore, a shoulder on the $\nu_{CH_2}^{assym}$ peak in Figure 1 could be detected in both samples at 2965−2962 cm^{-1}. This peak may be attributed to $\nu_{CH_3}^{assym}$ (the corresponding $\nu_{CH_3}^{sym}$ around 2870 cm^{-1} is likely too weak and overlapped by the $\nu_{CH_2}^{assym}$ and $\nu_{CH_2}^{sym}$ peaks to be clearly identified). The presence of CH_3 groups at the surface may be assigned to alkyl moieties of *N*-acylurea byproduct in water and unreacted *O*-acylurea in THF.

The 1430 cm^{-1} peak may be assigned to δ_{OH}^{COOH}. Another contribution to this peak could come from $\nu_{O=C-O-}^{sym}$ of carboxylates (the corresponding $\nu_{O=C-O-}^{assym}$ at ca. 1580 cm^{-1} is hardly detected due to the dipole's orientation to the surface). Deprotonation of carboxylic acids occurs as they interact with the carbodiimide. This peak's important decrease in THF from 8 to 24 h is not translated into an increase in NHS-ester but rather an increase in $\nu_{CH_3}^{sym}$ and $\nu_{CH_3}^{assym}$ which would suggest a higher conversion of COOH to unreacted *O*-acylurea.

Eventually, a peak at 1170 cm^{-1} is present in Figure 1 whose interpretation is uncertain.

OUTLOOK

NHS activation with different solvents and carbodiimides at different concentrations has been investigated by PM-IRRAS and ToF-SIMS. Our results show that, though the common procedure of activation in water with EDC/NHS does indeed lead to rapid esterification of the carboxylic acids even at 20 mM concentration, these activated esters are very unstable and rapidly hydrolyzed. Their presence could barely be detected after 24 h by the 1818 cm^{-1} and the m/z = 98 peaks (PM-IRRAS and ToF-SIMS, respectively). Furthermore, especially at high concentrations of EDC and NHS, significant amounts of *N*-acylurea byproduct may be formed, as suggested by the infrared amide I and II bands as well as CH_3NH^+ and $C_4H_6NO^+$ ToF-SIMS peaks. Moreover, an important increase in the 1650 cm^{-1} band between 8 and 24 h suggests the contribution of adsorbed water (increase in hydrophilicity of the surface).

In contrast, activation conducted in THF with DIC requires higher concentrations of carbodiimide and NHS and longer times but is more stable and does not form *N*-acylurea. However, it seems that unreacted *O*-acylurea remained after 24 h, as evidenced by the methyl band at 2965−2962 cm^{-1}.

ASSOCIATED CONTENT

Supporting Information

Summary of the most relevant vibrational modes and wavenumbers and evidence of lower deprotonation of MUA on aqueous ethanol than on pure ethanol. This material is available free of charge via the Internet at http://pubs.acs.org.

AUTHOR INFORMATION

Corresponding Authors

*E-mail: yann.chevolot@ec-lyon.fr.
*E-mail: jean-pierre.cloarec@ec-lyon.fr.

Notes

The authors declare no competing financial interest.

ACKNOWLEDGMENTS

The ANR P2N, ANR-12-NANO-0016-04 (PIRANEX project), is greatly acknowledged for financial support; CNANO Rhône-Alpes is acknowledged for PM-IRRAS funding; NanoLyon is acknowledged for providing gold samples; and CNRS and École Centrale de Lyon are acknowledged for JP Cloarec delegation in LN2. We also thank Thomas Géhin for technical support with PM-IRRAS characterization.

REFERENCES

(1) Afara, N.; Omanovic, S.; Asghari-Khiavi, M. Functionalization of a gold surface with fibronectin (FN) covalently bound to mixed alkanethiol self-assembled monolayers (SAMs): The influence of SAM composition on its physicochemical properties and FN surface secondary structure. *Thin Solid Films* **2012**, *522*, 381−389.

(2) Briand, E.; Salmain, M.; Compère, C.; Pradier, C.-M. Anti-rabbit immunoglobulin G detection in complex medium by PM-RAIRS and QCM Influence of the antibody immobilisation method. *Biosens. Bioelectron.* **2007**, *22*, 2884−2890.

(3) Choi, S.; Chae, J. Methods of reducing non-specific adsorption in microfluidic biosensors. *J. Micromech. Microeng.* **2010**, *20*, 075015.

(4) Morel, A.-L.; Volmant, R.-M.; Méthivier, C.; Krafft, J.-M.; Boujday, S.; Pradier, C.-M. Optimized immobilization of gold nanoparticles on planar surfaces through alkyldithiols and their use to build 3D biosensors. *Colloids Surf., B* **2010**, *81*, 304−312.

(5) Kim, I.; Junejo, I.-u.-R.; Lee, M.; Lee, S.; Lee, E. K.; Chang, S.-I.; Choo, J. SERS-based multiple biomarker detection using a gold-patterned microarray chip. *J. Mol. Struct.* **2012**, *1023*, 197−203.

(6) Bellon, S.; Buchmann, W.; Gonnet, F.; Jarroux, N.; Anger-Leroy, M.; Guillonneau, F.; Daniel, R. Hyphenation of surface plasmon resonance imaging to matrix-assisted laser desorption ionization mass spectrometry by on-chip mass spectrometry and tandem mass spectrometry analysis. *Anal. Chem.* **2009**, *81*, 7695−7702.

(7) El Khoury, G.; Laurenceau, E.; Chevolot, Y.; Souteyrand, E.; Cloarec, J.-P. A generic surface chemistry for peptide microarrays implementation: application to the detection of anti-H3 antibody. *Biosens. Bioelectron.* **2010**, *26*, 1320−1325.

(8) Campos, M. a. C.; Trilling, A. K.; Yang, M.; Giesbers, M.; Beekwilder, J.; Paulusse, J. M. J.; Zuilhof, H. Self-assembled functional organic monolayers on oxide-free copper. *Langmuir* **2011**, *27*, 8126−8133.

(9) Sam, S.; Touahir, L.; Salvador Andresa, J.; Allongue, P.; Chazalviel, J.-N.; Gouget-Laemmel, a. C.; Henry de Villeneuve, C.; Moraillon, a.; Ozanam, F.; Gabouze, N.; Djebbar, S. Semiquantitative study of the EDC/NHS activation of acid terminal groups at modified porous silicon surfaces. *Langmuir* **2010**, *26*, 809−814.

(10) Wang, C.; Yan, Q.; Liu, H.-B.; Zhou, X.-H.; Xiao, S.-J. Different EDC/NHS activation mechanisms between PAA and PMAA brushes and the following amidation reactions. *Langmuir* **2011**, *27*, 12058−12068.

(11) Touahir, L.; Chazalviel, J.-N.; Sam, S.; Moraillon, A.; Henry de Villeneuve, C.; Allongue, P.; Ozanam, F.; Gouget-Laemmel, A. C. Kinetics of Activation of Carboxyls to Succinimidyl Ester Groups in Monolayers Grafted on Silicon: An in Situ Real-Time Infrared Spectroscopy Study. *J. Phys. Chem. C* **2011**, *115*, 6782−6787.

(12) Briand, E.; Salmain, M.; Compère, C.; Pradier, C.-M. Immobilization of Protein A on SAMs for the elaboration of immunosensors. *Colloids Surf., B* **2006**, *53*, 215−224.

(13) Arima, Y.; Iwata, H. Effects of surface functional groups on protein adsorption and subsequent cell adhesion using self-assembled monolayers. *J. Mater. Chem.* **2007**, *17*, 4079−4087.

(14) Frey, B. L.; Corn, R. M. Covalent Attachment and Derivatization of Poly(L-lysine) Monolayers on Gold Surfaces As Characterized by Polarization-Modulation FT-IR Spectroscopy. *Anal. Chem.* **1996**, *68*, 3187−3193.

(15) Yang, Z.; Chevolot, Y.; Géhin, T.; Solassol, J.; Mange, A.; Souteyrand, E.; Laurenceau, E. Improvement of protein immobilization for the elaboration of tumor-associated antigen microarrays: application to the sensitive and specific detection of tumor markers from breast cancer sera. *Biosens. Bioelectron.* **2013**, *40*, 385−392.

(16) Papisov, M.; Maksimenko, a.V.; Torchilin, V. Optimization of reaction conditions during enzyme immobilization on soluble carboxyl-containing carriers. *Enzyme Microb. Technol.* **1985**, *7*, 11−16.

(17) Lockett, M. R.; Phillips, M. F.; Jarecki, J. L.; Peelen, D.; Smith, L. M. A tetrafluorophenyl activated ester self-assembled monolayer for the immobilization of amine-modified oligonucleotides. *Langmuir* **2008**, *24*, 69−75.
(18) Lei, Q. P.; Lamb, D. H.; Shannon, A. G.; Cai, X.; Heller, R. K.; Huang, M.; Zablackis, E.; Ryall, R.; Cash, P. Quantification of residual EDU (N-ethyl-N′-(dimethylaminopropyl) carbodiimide (EDC) hydrolyzed urea derivative) and other residual by LC-MS/MS. *J. Chromatogr., B* **2004**, *813*, 103−112.
(19) Methivier, C.; Beccard, B.; Pradier, C. M. In Situ Analysis of a Mercaptoundecanoic Acid Layer on Gold in Liquid Phase, by PM-IRAS. Evidence for Chemical Changes with the Solvent. *Langmuir* **2003**, *19*, 8807−8812.
(20) Schweiss, R.; Welzel, P. B.; Werner, C.; Knoll, W. Dissociation of Surface Functional Groups and Preferential Adsorption of Ions on Self-Assembled Monolayers Assessed by Streaming Potential and Streaming Current Measurements. *Langmuir* **2001**, *17*, 4304−4311.
(21) Schweiss, R.; Werner, C.; Knoll, W. Impedance spectroscopy studies of interfacial acid-base reactions of self-assembled monolayers. *J. Electroanal. Chem.* **2003**, *540*, 145−151.
(22) Schweiss, R.; Pleul, D.; Simon, F.; Janke, A.; Welzel, P. B.; Voit, B.; Knoll, W.; Werner, C. Electrokinetic Potentials of Binary Self-Assembled Monolayers on Gold: Acid-Base Reactions and Double Layer Structure. *J. Phys. Chem. B* **2004**, *108*, 2910−2917.
(23) Buffeteau, T.; Desbat, B.; Turlet, J. M. Polarization Modulation FT-IR Spectroscopy of Surfaces and Ultra-thin Films: Experimental Procedure and Quantitative Analysis. *Appl. Spectrosc.* **1991**, *45*, 380−389.
(24) Frey, B.; Corn, R.; Weibel, S. Polarization-Modulation Approaches to Reflection-Absorption Spectroscopy. *Hand. Vib. Spectrosc.* **2001**, *2*, 1042−1056.
(25) Cheng, F.; Gamble, L. J.; Grainger, D. W.; Castner, D. G. X-ray Photoelectron Spectroscopy, Time-of-Flight Secondary Ion Mass Spectrometry, and Principal Component Analysis of the Hydrolysis, Regeneration, and Reactivity of N-Hydroxysuccinimide-Containing Organic Thin Films. *Anal. Chem.* **2007**, *79*, 8781−8788.